

Charging of Dust in the Presence of a Directed Photon Flux: Numerical Simulations

Wojciech J. Miloch^{1,2}), Sergey V. Vladimirov²), Hans L. Pécseli³) and Jan Trulsen¹)

¹*Institute of Theoretical Astrophysics, University of Oslo, N-0315 Oslo, Norway*

²*School of Physics, The University of Sydney, Sydney, NSW 2006, Australia*

³*Department of Physics, University of Oslo, N-0316 Oslo, Norway*

(Received: 25 August 2008 / Accepted: 19 January 2009)

The charging of conducting and insulating dust grains in flowing plasmas in the presence of a directed photon flux is studied using Particle-In-Cell numerical simulations. We analyze the charge on dust grains for different photon fluxes and different angles of the photon incidence with respect to the supersonic plasma flow direction. For conducting grains we find that the total charge can be effectively controlled by the photon flux. On insulating grains, an electric dipole moment associated with the photoemission develops. A positive dust charge and photoelectrons distort several of the properties of the plasma surrounding the dust particle, and electrons are no longer Boltzmann distributed locally. Our results are compared with the case obtained without photoemission. The analysis is carried out in two spatial dimensions, with electrons and ions treated as individual particles.

Keywords: dust, charging, photoemission, UV-light, particle-in-cell

1. Introduction

The studies of wakes behind charged objects in flowing plasmas are of interest for understanding the interactions between charged dust grains in plasmas. Usually, dust grains in plasma devices are charged negatively due to a high mobility of electrons. A characteristic feature, that is due to a plasma flow, is the region of an enhanced ion density in the wake [1, 2, 3]. In a space environment dust grains are exposed to radiation, and therefore the photoelectric effect should be also included in the analysis of dust charging [4]. Photoemission will change the total charge on the dust and the surface charge distribution and can lead to new types of interactions between dust grains. Structures comprising positively charged dust grains were already observed in experiments [5, 6]. The possibility of electric attraction between positively charged grains was also discussed [7, 8].

A theory describing the dust charging with photoemission in a self-consistent way is difficult to develop. In particular, photoelectrons can modify the plasma in the vicinity of dust. Eventually, the theories may consider over-simplified models [9]. Therefore, one should employ numerical simulations, which can account for non-linear and stochastic phenomena, and model the charging of the dust in plasma in a self-consistent way. Numerical simulations usually treat electrons as a Boltzmann distributed background [10, 11]. Here we present a more realistic model by including both background- and photoelectrons in the analysis.

2. Numerical Code

We use the numerical particle-in-cell (PIC) code from our previous studies [12, 3], which is modified

by including a photon flux and the photoelectric effect [13]. We consider collisionless plasmas in a two dimensional system in Cartesian coordinates. Both electrons and ions are treated as individual particles, with the ion to electron mass ratio $m_i/m_e = 120$, and the electron to ion temperature ratio $T_e/T_i = 100$, where $T_e = 0.18$ eV. The plasma density is $n = 10^{10} \text{ m}^{-2}$, and the plasma flow velocity is $v_d = 1.5 C_s$, with C_s denoting the speed of sound.

A massive, circular dust grain of radius of $r = 0.375$ in units of the electron Debye length λ_{De} is placed inside a simulation box of size of $50 \times 50 \lambda_{De}$. It is initially charged only by the collection of electrons and ions. For a perfectly insulating grain, a plasma particle hitting the dust surface remains at this position at all later times and contributes to the surface charge distribution. To model a small conductor in this work, the charge is redistributed equally on the dust surface at each time step. Details on this algorithm are given in [13].

A directed photon flux is switched on after approximately 40 ion plasma periods τ_i . At this time, we can assume that the surface charge distribution has reached a stationary level. Three different angles between the incoming photons and the direction of the ion drift are considered: $\alpha = \{0^\circ, 90^\circ, 180^\circ\}$. For a conducting dust, the simulated photon flux is $\Phi_{h\nu} \in (0.25, 2.5) \times 10^{19} \text{ m}^{-2}\text{s}^{-1}$ with photon energies $E_{h\nu}$ of 4.8 and 5.5 eV. These photon parameters can be achieved by commercially produced UV lamps (e.g., low pressure mercury lamps) [14]. The work function W of the conducting dust grains is $W = 4.5$ eV, which is close to work functions of many metallic materials [15]. For an insulating dust, the photon energies $E_{h\nu}$ are 10.3 and 11.0 eV, and the

author's e-mail: wojciecm@astro.uio.no

$\Phi_{h\nu}$ ($10^{19}\text{m}^{-2}\text{s}^{-1}$)	$E_{h\nu} = 4.8 \text{ eV}$		$E_{h\nu} = 5.5 \text{ eV}$	
	q_t (q_0)	Δq_t (%)	q_t (q_0)	Δq_t (%)
0.0	-752	4	-752	4
0.25	-163	19	-168	17
0.50	19	173	12	258
1.25	251	18	273	18
2.50	795	8	1330	7

Table 1 The averaged total charge q_t and relative charge fluctuations Δq_t on the conducting dust grain for different photon energies $E_{h\nu}$ and different photon fluxes $\Phi_{h\nu}$ for $\alpha = 0^\circ$.

work function is $W = 10 \text{ eV}$.

When a photon hits the dust, a photoelectron of energy $E = E_{h\nu} - W$ is produced at distance $l = sv\Delta t$ from the dust surface, where s is an uniform random number $s \in (0, 1]$, Δt is the computational time step and v is the photoelectron speed. Photoelectron velocity vectors are uniformly distributed over an angle of π and directed away from the dust surface. The code is run typically up to 50 ion plasma periods.

3. Results

With the onset of the photon flux, the charge on the conducting dust grain becomes more positive, and it reaches a saturation level within one ion plasma period. The saturation charge, averaged over a time interval of nine ion plasma periods, is summarized in Table 1 and presented in units of the elementary two dimensional charge: $q_0 = e [n_{0(3D)}]^{1/3}$, where e is an elementary charge, and $n_{0(3D)}$ is the plasma density in the three dimensional system. For a sufficiently high photon flux, the dust is positively charged. For low fluxes, the saturation charge does not depend on the photon energy. For higher fluxes, photoelectrons with higher energies lead to a more positive dust grain. The relative fluctuations of the charge are largest for the dust with lower charge. The absolute and relative charge fluctuations are smallest for the case without photoemission.

For low photon fluxes we observe the ion focusing, which is weaker than for the case without the photoemission. The ion focusing is destroyed for positively charged grains. In this case, ions are slowed down in front of the grain and deflected by the dust. Consequently, the region of an enhanced ion density can be formed in front of the grain, while downstream from the grain a distinct boundary between the wake and the undisturbed plasma is present. This can be inferred from Fig. 1 where the ion density around a conducting grain is shown for $\alpha = 0^\circ$.

The wake in the ion density, which we refer to as the region where the density is reduced by more than 50% with respect to the undisturbed ion density, scales behind a conducting dust with the photon flux

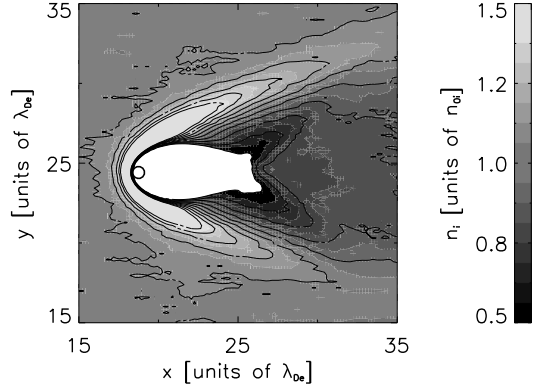


Fig. 1 The ion density around the dust grain exposed to the photon flux $\Phi_{h\nu} = 2.5 \cdot 10^{19} \text{ m}^{-2}\text{s}^{-1}$ of energy $E_{h\nu} = 4.8 \text{ eV}$ averaged over nine ion plasma periods τ_i . $\alpha = 0^\circ$ and the plasma flow is in the positive x direction. The white region corresponds to ion densities below $0.5n_{0i}$.

$\Phi_{h\nu}$ ($10^{19}\text{m}^{-2}\text{s}^{-1}$)	$E_{h\nu} = 4.8 \text{ eV}$		$E_{h\nu} = 5.5 \text{ eV}$	
	w (λ_{De})	d (λ_{De})	w (λ_{De})	d (λ_{De})
0.50	0.7	3.1	0.7	3.5
1.25	2.1	6.8	2.3	7.5
2.50	3.6	7.0	5.9	11.1

Table 2 The width w and length d of the ion wake behind a positively charged dust grains for different photon energies $E_{h\nu}$ and different photon fluxes $\Phi_{h\nu}$ for $\alpha = 0^\circ$. The ion wake was not observed for $\Phi_{h\nu} < 0.5 \cdot 10^{19} \text{ m}^{-2}\text{s}^{-1}$

and photon energy, being larger for higher fluxes and energies. The measured spatial extent of the wake is summarized in Table 2. The ion wake corresponds to the white region behind the dust in Fig. 1.

The potential around the positively charged conducting dust becomes polarized for higher photon fluxes. In Fig. 2, the potential distribution around the conducting dust is shown for different angles of incidence of photons with the high flux. The polarization of the plasma is the largest for $\alpha = 180^\circ$. Here the potential is negative behind, and positive in front of the dust.

For the case of an insulating grain, we observe the charge saturation for lower photon fluxes, when the total charge on the dust remains negative. For fluxes high enough to change the sign of the total dust charge, the charge does not saturate. In all cases, the charging depends on the angle of incidence, see Fig. 3. For lower fluxes the charge is less negative for larger α . For higher fluxes, the charge can become positive, and then negative within a few ion plasma periods. This is not the case for $\alpha = 180^\circ$, where the charge is getting more positive. Here, the positive surface charge on the shadow side can not be balanced by the electron current because of the development of a

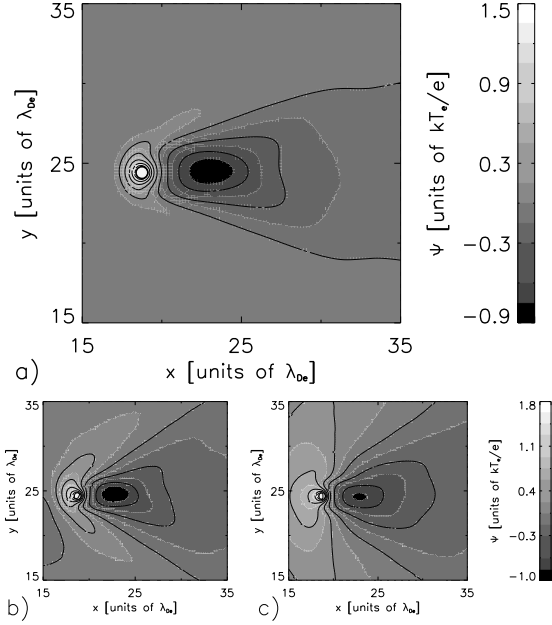


Fig. 2 The averaged potential around the dust grain exposed to the photon flux $\Phi_{h\nu} = 2.5 \cdot 10^{19} \text{ m}^{-2} \text{ s}^{-1}$ of energy $E_{h\nu} = 4.8 \text{ eV}$ and for $\alpha = 0^\circ$ (a), $\alpha = 90^\circ$ (b), and $\alpha = 180^\circ$ (c).

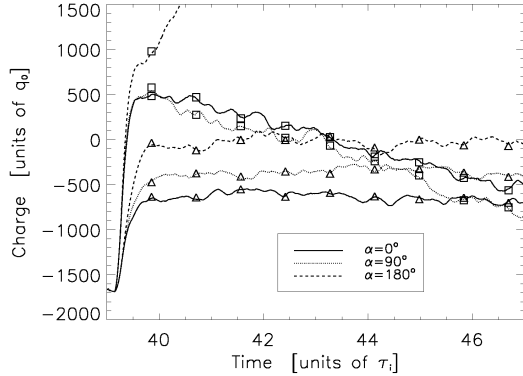


Fig. 3 The total charge on the insulating dust grain as a function of time for different photon fluxes and angles of photon incidence α . Squares correspond to the photon flux $\Phi_{h\nu} = 2.5 \cdot 10^{19} \text{ m}^{-2} \text{ s}^{-1}$, while triangles to $\Phi_{h\nu} = 0.5 \cdot 10^{19} \text{ m}^{-2} \text{ s}^{-1}$. The photon energy is $E_{h\nu} = 11.0 \text{ eV}$. The results are smoothed with the moving box average filter for presentation.

strong electric dipole moment antiparallel to the ion flow and the electron and ion density wakes behind the grain.

The ion density and potential distributions around an insulating grain evolve in time. For a positively charged dust, the ion focusing region in the wake is destroyed, and the wake behind the dust with $\alpha = 0^\circ$ is similar to the case of the conductor. However, when the charge is negative again, the wake becomes smaller, and the ion focus can be retrieved, see Fig. 4. The wake is strongly asymmetric for $\alpha = 90^\circ$. This asymmetric charge distribution is present also

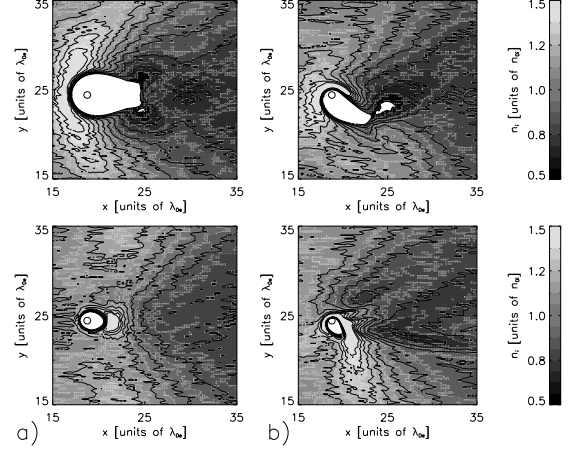


Fig. 4 The ion density around insulating dust grains exposed to the photon flux $\Phi_{h\nu} = 2.5 \cdot 10^{19} \text{ m}^{-2} \text{ s}^{-1}$, $\alpha = 0^\circ$ (a) and $\alpha = 90^\circ$ (b) of energy $E_{h\nu} = 11.0 \text{ eV}$ averaged over two ion plasma periods: $t \in (39.5, 41.5)\tau_i$ (top) and $t \in (48.0, 50.0)\tau_i$ (bottom).

after the closure of the wake, see Fig. 4b).

With the onset of the photon flux, we observe the development of an electric dipole moment on the insulating dust surface which is antiparallel to the direction of incident photons. This electric dipole moment does not saturate for large photon fluxes, and it is larger than the electric dipole moment due to the ion flow.

In Fig. 5, we illustrate the difference δ between the density of Boltzmann distributed electrons that would correspond to the calculated potential and the actual electron density: $\delta = n_{e0} \exp[-e\Psi/kT_e] - n_e$, where $e < 0$ is the electron charge. Before the onset of the photon flux the electrons can be well approximated by the Boltzmann distribution. With photoemission, the electrons are no longer Boltzmann distributed. The largest discrepancies for conductors are associated with the surplus of electrons due to the photoelectron emission, and to the region of the enhanced ion density in front of the dust, where electrons are underrepresented. For insulators the electric dipole governs the potential in vicinity of the dust.

4. Discussion

The photoemission provides an electron source on the side of the photon incidence. Photoelectrons localized in the vicinity of dust surface are being attracted by the positively charged dust grain and redistributed as to cancel the positive charge region in front of the dust. If the photoelectron energy is lower or comparable to the electron thermal velocity, the electron can easily be lost on the dust surface, while electrons with larger energies are more likely to escape. This, together with the photoemission rate, which is proportional to the photon flux, explains the higher positive charge on the dust for high energetic photons and high

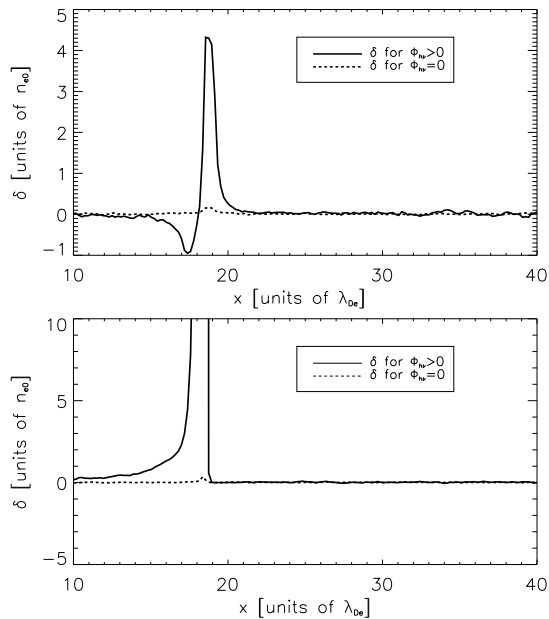


Fig. 5 The difference δ between the density of Boltzmann distributed electrons that would correspond to the calculated potential and the actual electron density is shown for both cases (dashed line - without, solid line - with photoemission). Both conducting (top) and insulating (bottom) dust grains are considered for $\alpha = 0^\circ$.

fluxes.

The electron density is reduced in the region corresponding to the ion wake, but it is still large enough to give rise to the negative potential region behind a positively charged dust, see Fig. 2. This potential enhancement is more pronounced than the one associated with the ion focusing behind the negatively charged grain, and may lead to strong interactions between positively charged particles along the ion flow. A positive potential region can develop in front of the dust, provided the local electron density is insufficient to fully neutralize the enhancement in the ion density. In this case, the plasma becomes polarized and can have an associated electric dipole moment. The highest polarization degree is found for $\alpha = 180$.

The region of the reduced ion density behind a positively charged conducting grain scales with the photon flux and photon energy. The ion density wake behind a positively charged insulating grain changes in time, and the ion focusing can be recovered when the total charge on the grain becomes negative. In certain parameter regime, the depletion in the ion density due to absorption can have important implications. In particular, it can lead to a superfluidlike motion of dust grains in plasma [16].

The UV radiation allows for an accurate control of the charge on a metallic dust grain in plasma devices. By an appropriate flux selection the coagulation of small dust grains can be induced due to their large fluctuations in the total charge in the presence of the

photon flux. The photoemission should also allow to manipulate the height of a dust grain levitated in the sheath of dc discharges.

For insulators, the charge control is more difficult, because of the development of the electric dipole moment which direction depends on the angle of photon incidence on the dust surface. With $\alpha = 180^\circ$ the saturation of the charge is not observed within the simulation time, while for other angles the charge recovers to negative values. Rotation of dust can redistribute the surface charge on the dust surface and make it more even. The analysis of the rotating insulating grain can resemble the case for conductors. The rotation of the dust was not simulated in the present work.

Finally, it was shown that with the photoemission, the electrons have non-Boltzmann distribution, which makes solely theoretical analysis of the problem difficult.

This work is supported in part by the Norwegian Research Council (NFR) and in part by the Australian Research Council (ARC).

- [1] S. V. Vladimirov and M. Nambu, *Phys. Rev. E*, **52**, R2172 (1995).
- [2] S. A. Maiorov, S. V. Vladimirov and N. F. Cramer, *Phys. Rev. E*, **63**, 017401 (2000).
- [3] W. J. Miloch, H. L. Pécseli and J. Trulsen, *Phys. Rev. E*, **77**, 056408 (2008).
- [4] M. Horányi, *Annu. Rev. Astro. Astrophys.*, **34**, 383 (1996).
- [5] V. E. Fortov *et al.*, *JETP*, **87**, 1087 (1998).
- [6] A. A. Samarian and O. S. Vaulina, *Phys. Lett. A*, **278**, 146 (2000).
- [7] G. L. Delzano, G. Lapenta and M. Rosenberg, *Phys. Rev. Lett.*, **92**, 035002 (2004).
- [8] S. A. Khrapak, G. E. Morfill, V. E. Fortov, L. G. D'yachkov, A. G. Khrapak, and O. F. Petrov, *Phys. Rev. Lett.*, **99**, 055003 (2007).
- [9] K. Ostrikov, M. Y. Yu and L. Stenflo, *IEEE Trans. Plasma Sci.*, **29**, 175 (2001).
- [10] E. Engwall, A. I. Eriksson and J. Forest, *Phys. Plasmas*, **13**, 062904 (2006).
- [11] V. Land and W. J. Goedheer, *IEEE Trans. Plasma Sci.*, **35**, 280 (2007).
- [12] W. J. Miloch, H. L. Pécseli and J. Trulsen, *Nonlin. Processes Geophys.*, **14**, 575 (2007).
- [13] W. J. Miloch, S. V. Vladimirov, H. L. Pécseli and J. Trulsen, *Phys. Rev. E*, **77**, 065401(R) (2008).
- [14] K. F. McDonald, R. D. Curry and P. J. Hancock, *IEEE Trans. Plasma Sci.*, **30**, 1986 (2002).
- [15] M. Rosenberg, A. Mendis and D. P. Sheehan, *IEEE Trans. Plasma Sci.*, **24**, 1422 (1996).
- [16] S. V. Vladimirov, S. A. Khrapak, M. Chaudhuri, and G. E. Morfill, *Phys. Rev. Lett.*, **100**, 055002 (2008).